Acta Cryst. (1994). B50, 644–648

Lattice Constants and Thermal Expansion of H_2O and D_2O Ice I*h* Between 10 and 265 K

BY K. RÖTTGER, A. ENDRISS AND J. IHRINGER

Institut für Kristallographie, Universität Tübingen, Charlottenstrasse 33, D-72070 Tübingen, Germany

S. DOYLE

Hasylab/DESY, Notkestrasse 85, D-22603 Hamburg, Germany

AND W. F. KUHS*

Mineralogisch-Kristallographisches Institut, Universität Göttingen, Goldschmidtstrasse 1, D-37077 Göttingen, Germany

(*Received* 23 *March* 1994; *accepted* 6 *May* 1994)

In memoriam Akira Goto (1963–1992)

Abstract

The lattice constants of powdered H_2O and D_2O ice I*h* were measured in the temperature range 10–265 K with synchrotron radiation to a precision of typically 0.003% in *a* and 0.007% in *c*. The *c*/*a* ratio remains almost constant with temperature, thus the thermal expansion is virtually isotropic. Below 73 K, one observes a negative thermal expansion for both light and heavy ice I*h*. The temperature dependency of the thermal expansion at higher temperatures follows roughly that of the specific heat. Thus, the Grüneisen function is negative at low temperatures and is slowly varying above 120 K; the isotopic differences of the Grüneisen function are smaller than previously assumed.

1. Introduction

The thermal expansion of ice I*h* (space group: $P6_3/mmc$) has been measured repeatedly by dilatometric and X-ray techniques since the first experiments close to the melting point by Struve (1845). Jakob & Erk (1929) measured dilatometrically the thermal expansion down to temperatures of 20 K on long polycrystalline ice cylinders and found a negative thermal expansion below 70 K. Early X-ray powder work did not cover the full temperature range (Barnes, 1929; Megaw, 1934; Vegard & Hillesund, 1942) and later work added only lattice constants at a few selected temperatures (Truby, 1955; Blackman & Lisgarten, 1957). Lonsdale (1958) attempted a combination of the various data and concluded that ice I*h* exhibits an increasingly anisotropic thermal expansion at decreasing temperatures. This unexpected result led LaPlaca & Post (1960) to a reinvestigation and to the discovery of anomalous behaviour near 120 K, which was attributed to precursors of an inhibited disorder–order transition. Later measurements by Brill & Tippe (1967) could not confirm this anomaly, while unpublished work by Haltenorth (1973) supported it in HF-doped samples. The negative thermal expansion found in the early dilatometric work was never confirmed by X-ray methods, but was corroborated in single-crystal experiments by Dantl (1962). Likewise, a temperature dependency of the *c*/*a* ratio (and thus an anisotropy of thermal expansion) was claimed by several authors, although never established unambiguously. Therefore, considerable uncertainties prevailed until recently. The situation was even worse for a quantitative assessment of the isotopic difference between normal and heavy ice I*h*; the scarce and incoherent data did not permit any definite statement on the D_2O lattice constants, except that they were considered larger than those of H_2O (Lonsdale, 1958; Kuhs & Lehmann, 1986). Table 1 gives an account of samples and techniques used, the temperature ranges covered and the precisions achieved in some of the earlier work. A reinvestigation therefore seemed appropriate also in view of an urgent need for lattice constant data for both H_2O and D_2O in order to elucidate structural differences between the isotopic compounds (Kuhs & Lehmann, 1987). High-resolution powder diffraction using synchrotron radiation was considered appropriate to clarify the situation.

2. Experimental

The lattice constants of ice I*h* for H_2O and D_2O were measured at the synchrotron radiation laboratory, Hasylab at DESY/Hamburg, with the powder diffractometer in parallel beam geometry (Arnold *et al.*, 1989). For relatively thick samples (as were the ice samples in our case), this geometry is especially well suited, because sample position and thickness do not affect the measured diffraction angles. In order to obtain a homogenous and

*Author to whom correspondence should be addressed.

Table 1. *Summary of experimental work*

Authors	Method	Sample	T range (K)	Isotopes	Precision (lattice const.) (%)
Jacob & Erk (1929)	Dilatometry	Polycrystal	23–273	H	
Megaw (1934)	X-ray	SC	207 + 273	H,D	0.05
LaPlaca & Post (1960)	X-ray	Powder	93–263	H	0.01
Dantl (1962)	Dilatometry	SC	20–270	H,D	
Brill & Tippe (1967)	X-ray	Powder	13–193	H	0.01
Haltenorth (1973)	Neutron	HF-doped SC	88–228	H	0.002
This work	Synchrotron	Powder	10–265	H,D	0.003 in *a* 0.007 in *c*

finely ground powder of ice I*h*, the sample must be prepared below 270 K and kept below this temperature during the transfer to the cryostat. Thus, the preparation was performed at a temperature of *ca* 220 K in a partly covered nitrogen-cooled polystyrene box standing near the diffractometer. The nitrogen atmosphere prevented the condensation of water from the air, and the manipulations were performed with gloves. A drop of water (H_2O: doubly distilled and degassed; D_2O: 99.9 atom% from Aldrich Chemical Co.) was syringed on top of a precooled flat teflon plate and splashed by a pistil. With a precooled mortar, the ice sheets obtained were easily ground to a fine powder, which was mixed with the NBS-standard powder of silicon (640*b*). The powdered sample was placed into the precooled holder between two polyethylene foils. At the same time, the head of the opened cryostat (Ihringer & Kuester, 1993) was cooled by boiling nitrogen, kept in a special insulating box placed around the cryostat head. This allowed the setting of the sample holder to its assigned position and to assemble the cryostat without melting the sample.

Three silicon and 11 ice reflections were measured at scattering angles between 18 and 62° in the temperature range 265–10 K at intervals of 15 K with the following conditions: stepsize (2θ) 0.004 for the 100 and 101 reflections, 0.006 for intermediate scattering angles and 0.008 for the 300 and 213 reflections; typically, 15 steps per reflection, 10 000 cts in monitor corresponding to 2–8 s acquisition time per step; DORIS operation with injection to 80 mA every 3–4 h. The calibrated wavelength was 1.2873 Å at the beginning and 1.2884 Å at the end of the data collection; a correction for this variation is described below. The reflections chosen (see Table 2) had no overlap with other reflections; their peak shapes were in good agreement with a Gaussian. To obtain a good thermal contact with the sample during the measurements, the cryostat sample chamber was filled with helium gas at a pressure of *ca* 100 Torr. The amount of helium entering the ice lattice at this pressure is negligible (Kahane, Klinger & Philippe, 1969). The temperature was controlled to within < 0.5 K. After the data collection with a stepwise cooling down to 10 K, the sample was remeasured at 250 K to check the diffractometer and sample settings; no significant deviations from the first set of data obtained prior to cooling were detected; a final data set was collected at 265 K.

Table 2. *Measured ice* I*h and silicon reflections at* 250 K

	hkl	2θ (H_2O)	FWHM	2θ (D_2O)	FWHM
1	100	18.8765 (1)	0.0210 (2)	18.8632 (1)	0.0225 (2)
2	101	21.4189 (1)	0.0155 (2)	21.4028 (1)	0.0177 (3)
3	Si, 111	23.6364 (3)	0.0227 (7)	23.6378 (4)	0.0210 (8)
4	102	27.7393 (1)	0.0193 (3)	27.7182 (2)	0.0207 (4)
5	110	33.0547 (2)	0.0292 (4)	33.0320 (4)	0.0335 (7)
6	103	36.0375 (3)	0.0374 (6)	36.0129 (4)	0.0390 (7)
7	020	38.3631 (4)	0.0418 (8)	38.3421 (6)	0.0459 (12)
8	202	43.7107 (9)	0.0624 (21)	43.6751 (11)	0.0613 (25)
9	Si, 311	46.2463 (4)	0.0785 (9)	46.2558 (7)	0.0799 (15)
10	203	49.7352 (8)	0.0760 (17)	49.6973 (10)	0.0725 (25)
11	210	51.5609 (19)	0.0920 (54)	51.5188 (14)	0.0879 (36)
12	300	59.0899 (21)	0.0999 (64)	59.0673 (18)	0.1042 (44)
13	213	61.0359 (43)	0.1410 (99)	61.0085 (22)	0.1284 (76)
14	Si, 331	62.1681 (20)	0.1333 (72)	62.1825 (22)	0.1406 (55)

3. Data analysis

The measured profiles of all 14 reflections were fitted by a Gaussian without asymmetry correction; the weighted profile R-values were typically 0.08. The obtained line positions and their standard deviations were used to calculate the lattice constants of H_2O and D_2O for all temperatures (see Table 3). It turned out to be essential to correct for the wavelength changes caused by thermal expansion of the monochromator crystals and/or by changes in the incident beam position during the measurements. Therefore, the line positions of ice I*h* were calibrated for each temperature using the silicon reflections. For the calibration at temperatures above 190 K, an equation given by Okada & Tokumaru (1984) was used; below 190 K the calibration was carried out using the experimental expansivity data of Lyon, Salinger & Swenson (1977).

The lattice constants of ice I*h* *versus* temperature are shown in Figs. 1 and 2. At all temperatures, the D_2O lattice constants are significantly larger than those for H_2O. Below 75 K, a negative thermal expansion coefficient is detected for both isotopes. The *c*/*a* ratio shows no significant variation with temperature. Fig. 3 exhibits the temperature dependency of the volume of the unit cell. Physics requires a vanishing expansivity at 0 K ($\lim_{T\to 0\,K}\ \alpha = 0$) and a horizontal tangent at 0 K

Table 3. *Lattice constants of* H_2O *and* D_2O *ice* I*h*

No.	T (K)	$a(H_2O)$	$c(H_2O)$	$a(D_2O)$	$c(D_2O)$
18	265	4.52141 (20)	7.36163 (59)	4.52662 (42)	7.36882 (134)
19	250	4.51842 (46)	7.35556 (138)	4.52243 (44)	7.36265 (152)
1	250	4.51808 (11)	7.35612 (34)	4.52154 (10)	7.36270 (32)
2	235	4.51480 (14)	7.35027 (50)	4.51805 (28)	7.35575 (90)
3	220	4.51168 (17)	7.34472 (65)	4.51455 (13)	7.35084 (39)
4	205	4.50877 (10)	7.34109 (42)	4.51144 (13)	7.34596 (43)
5	190	4.50632 (09)	7.33722 (33)	4.50833 (14)	7.34123 (42)
6	175	4.50416 (26)	7.33317 (93)	4.50571 (20)	7.33692 (64)
7	160	4.50209 (22)	7.32959 (82)	4.50354 (22)	7.33343 (65)
8	145	4.50020 (12)	7.32678 (44)	4.50145 (15)	7.33028 (45)
9	130	4.49880 (14)	7.32397 (54)	4.50012 (9)	7.32674 (28)
10	115	4.49753 (15)	7.32194 (52)	4.49857 (20)	7.32502 (60)
11	100	4.49664 (16)	7.32044 (58)	4.49766 (24)	7.32284 (68)
12	85	4.49613 (14)	7.31976 (56)	4.49721 (20)	7.32201 (59)
13	70	4.49587 (12)	7.31985 (54)	4.49689 (34)	7.32265 (118)
14	55	4.49638 (19)	7.32003 (63)	4.49729 (21)	7.32157 (64)
15	40	4.49671 (25)	7.32049 (89)	4.49774 (23)	7.32264 (70)
16	25	4.49674 (19)	7.32052 (70)	4.49804 (21)	7.32292 (66)
17	10	4.49693 (22)	7.32109 (74)	4.49819 (17)	7.32348 (53)

($\lim_{T\to 0\,K} \delta\alpha/\delta T = 0$), thus in the polynomial to fit the volume at all experimental temperatures

$$V(T) = A_0 + A_1T + A_2T^2 ... + A_8T^8; \qquad (1)$$

the coefficients A_1 and A_2 had to be zero; the final non-zero coefficients are given in Table 4. Fig. 4 shows the linear thermal expansivity coefficient $\alpha = (1/3)\beta$, with the volume expansivity β given as

$$\beta = (1/V)(\partial V/\partial T) \qquad (2)$$

and being calculated for H_2O and D_2O by inserting the polynomial expression (1) and its derivative into (2). The unit-cell volume at the melting point was deduced from the literature values of the mass density [H_2O: 0.91671 Mg m^{-3} (Ginnings & Corruccini, 1947); D_2O: 1.01475 Mg m^{-3} (Timmermans, Hennaut-Roland & Rozental, 1936)]. Below 100 K, α is similar for H_2O and D_2O; above 100 K, the thermal expansivity becomes increasingly larger for D_2O.

4. Discussion

Bulk density, lattice constants and expansivity data of ice I*h* have been measured repeatedly with results often differing by multiples of the e.s.d.'s. Systematic errors must be the cause of these discrepancies and it is likely that they originate in the experimental techniques as well as in the samples used. A discussion of the effects of aging, ordering phenomena, impurities and cracks on the volume–temperature data is beyond the scope of this paper and a critical assessment of possible systematic errors in the published data is almost impossible. With this disclaimer in mind, a discussion of our results is thus attempted.

The lattice constants obtained for light and heavy ice I*h* show very similar behaviour as a function of temperature. The isotopic differences are highly significant and are somewhat larger than the values obtained from the single-crystal data by Megaw (1934). The lattice constants of D_2O are larger by a factor of 1.0010 (2) at 250 K, with decreasing differences at lower temperatures; below 70 K, the factor remains constant at a value of 1.0003 (1). The *c*/*a* ratio shows very little temperature variation; the only feature is a slight increase

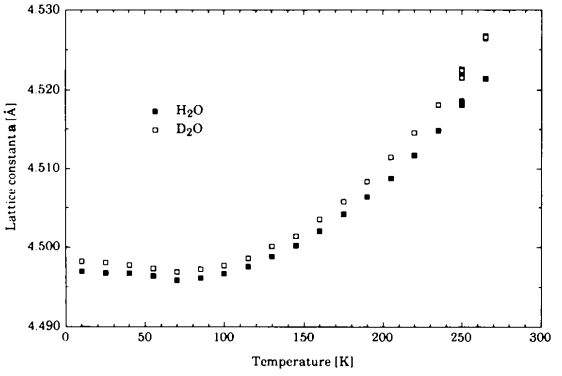

Fig. 1. Lattice constant *a* of ice I*h* between 10 and 265 K.

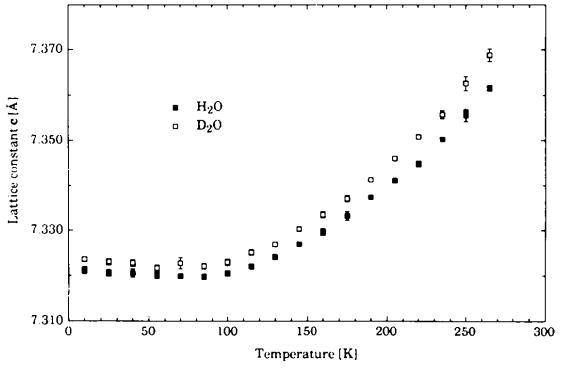

Fig. 2. Lattice constant *c* of ice I*h* between 10 and 265 K.

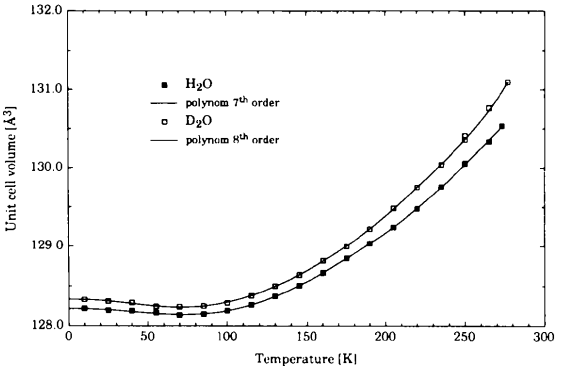

Fig. 3. Unit-cell volume of ice I*h* between 10 and 265 K; entries at the melting point derived from mass density (see text).

Table 4. *Coefficients and quality of polynomial fit to the unit-cell volume data**

	H_2O	D_2O
A_0	128.215 (16)	128.332 (15)
A_3	$-1.31\ (26) \times 10^{-6}$	$-2.26\ (65) \times 10^{-6}$
A_4	$2.48\ (52) \times 10^{-8}$	$5.16\ (1.77) \times 10^{-8}$
A_5	$-1.61\ (38) \times 10^{-10}$	$-4.58\ (1.91) \times 10^{-10}$
A_6	$4.61\ (1.26) \times 10^{-13}$	$2.09\ (1.01) \times 10^{-12}$
A_7	$-4.97\ (1.52) \times 10^{-16}$	$-4.86\ (2.64) \times 10^{-15}$
A_8	0	$4.57\ (2.69) \times 10^{-18}$
χ^2	6.91	6.12

* Uncertainties in parentheses correspond to 90% confidence level.

for D_2O above 70 K and a corresponding slightly larger c/a value for D_2O compared with H_2O [1.62806 (9) for H_2O and 1.62828 (12) for D_2O in the range 70–250 K]. There is no doubt that the c/a ratio is smaller than the theoretical value of 1.63299 for homogeneous packing. Using the extensive structural data (Kuhs & Lehmann, 1986, 1987), the deformation of the ideal packing is identified as a deviation of the O—O—O angles from their tetrahedral values; the O—O—O angles are wider when two of the O atoms are in the hexagonal plane, leading to a slight contraction along the c-axis. The time-space averaged O—O distances along and oblique to the c-axis are identical for each compound within the limit of error; however, there is a slight increase of the O—O distance on going from H_2O to D_2O, an increase which is commensurate with the increase in lattice constants. It should be mentioned that the isotope ratio of the molar volume of ice ($V_{m,D_2O}/V_{m,H_2O}$) close to the melting point (273 K) is smaller than in the liquid phase at 277 K (1.0033 and 1.0061, respectively). This means that compared with the situation in ice I*h*, the atomic arrangement of D_2O water becomes more open than that of H_2O water. This is consistent with the generally accepted picture that the arrangement of water molecules in heavy water is more 'structured' (has a smaller width of the distribution of hydrogen-bond distances and angles, as well as fewer broken hydrogen bonds) than in normal water (Kuharsky & Rossky, 1985; Root, Egelstaff & Hime, 1986). A similar quantum effect exists not only in water, but also in (the orientationally disordered) ice I*h*, although on a smaller scale (Kuhs & Lehmann, 1987). The increased difference in molar volume for H_2O and D_2O on going from the solid to the liquid phase should then be attributed to a relative loss of structure due to quantum effects in H_2O compared with D_2O.

The linear thermal expansion coefficients show a remarkable temperature dependency. Below 73 K, one observes a negative thermal expansion for H_2O and D_2O, in reasonable agreement with the work by Jakob & Erk (1929); the zero-expansivity temperature quoted by Dantl (1962) is located slightly lower at 63 K. A comparison with selected literature data is given in Fig. 5. Topologically similar tetrahedrally bonded structures, such as ZnS (Adenstedt, 1936), Si and InSb (Gibbons, 1958) or GaAs, ZnSe and Ge (Novikova, 1961), show similar behaviour. Lattice dynamical models have been developed for diamond, silicon and other III–V compounds to explain this effect in terms of a negative Grüneisen parameter of the transversal-acoustic phonons near the Brillouin-zone boundary (Blackman, 1958; Haruna, Maeta, Ohashi & Koike, 1986; Biernacki & Scheffler, 1989; Xu, Wang, Chan & Ho, 1991). A detailed lattice dynamical study for ice I*h*, which could explain its negative thermal expansion, has not yet been performed; thus, the mode(s) causing the effect is(are) not identified. However, the similarity of the expansivity of light and heavy ice I*h* at low temperature, together with the temperature range in which the negative expansion coefficients prevail, clearly suggests (a) translational mode(s) as the cause.

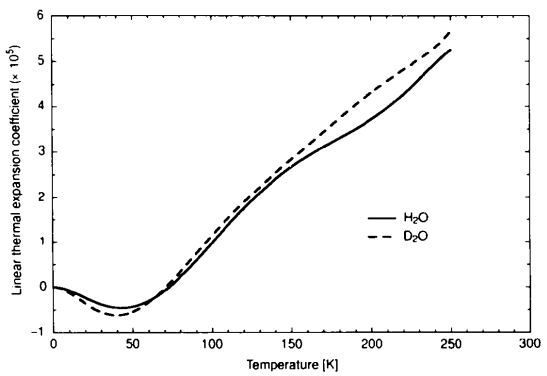

Fig. 4 . Linear thermal expansivity coefficient of ice I*h* calculated from the polynomial fits.

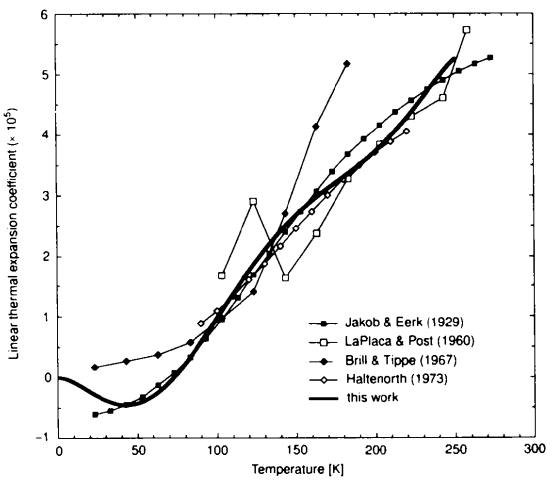

Fig. 5. Comparision of literature data on the linear thermal expansivity coefficient for H_2O ice I*h*. Note that the data by Haltenorth were obtained on a HF-doped crystal. Although doping is known to have a very small effect on the lattice constants at 227 K (Truby, 1955), its effect on the expansivity is not known exactly.

The expansivity data at higher temperatures show some further interesting features; for H_2O, the slope is steep up to approximately 140 K, followed by a flatter part up to approximately 200 K and a final steeper part up to the melting point. D_2O exhibits increasingly larger expansion coefficients with increasing temperature, with the flatter part of the curve shifted to higher temperatures and the final steep part setting in at 240 K. The entries close to the melting point must be considered with some caution as the lattice constant data in this region show somewhat larger errors. There is a close correlation of the H_2O expansivity data with the specific heat measured by Giauque & Stout (1936). Using a simple quasiharmonic model, one may calculate the Grüneisen function from the volume thermal expansion β, the adiabatic bulk modulus K, the specific heat C_p and the molar volume V_m as

$$\gamma_G(T) = (\beta K V_m)/C_p. \quad (3)$$

The D_2O specific heat data were taken from Long & Kemp (1936). The adiabatic bulk modulus is calculated from the elastic constant data of Dantl (1968) for H_2O and Mitzdorf & Helmreich (1971) for D_2O according to

$$K = (c_{11}+c_{12}+2c_{33}-4c_{13})/[c_{33}(c_{11}+c_{12})-2c_{13}^2]. \quad (4)$$

It should be mentioned that the elastic constant data were determined only in the temperature range above 133 K, introducing a slight uncertainity for the low-temperature values of the Grüneisen function. The specific heat at higher temperatures follows roughly the expansivity pattern, thus the calculated Grüneisen function shows a flatter part above approximately 120 K with a final increase on approaching the melting point (see Fig. 6) and only small differences between light and heavy ice. The isotopic differences are definitely smaller than those deduced from the tentative values of the individual Grüneisen functions given by Leadbetter (1965), obtained under the assumption of vanishing isotopic differences for expansivity and compressibility.

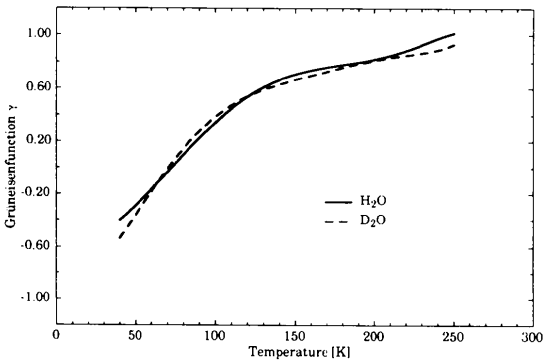

Fig. 6. Grüneisen function of ice *Ih* calculated between 40 and 250 K.

It is intriguing that the absolute magnitude and the temperature dependency of γ_G is very similar to that found in other tetrahedrally coordinated compounds (Collins & White, 1964), corroborating the analogies invoked in the discussion of the negative thermal expansion at low temperatures.

We acknowledge the financial support by the DFG under project IH 9/3-1 and the BMFT. We thank Professor W. Prandl for stimulating and helpful discussions.

References

ADENSTEDT, H. (1936). *Ann. Phys.* **26**, 69–96.
ARNOLD, H., BARTL, H., FUESS, H., IHRINGER, J., KOSTEN, K., LÖCHNER, U., PENNARTZ, P. U., PRANDL, W. & WROBLEWSKI, T. (1989). *Rev. Sci. Instrum.* **60**, 2380–2381.
BARNES, W. H. (1929). *Proc. R. Soc. A*, **125**, 670–693.
BIERNACKI, S. & SCHEFFLER, M. (1989). *Phys. Rev. Lett.* **63**, 290–293.
BLACKMAN, M. (1958). *Philos. Mag.* **9**, 831–838.
BLACKMAN, M. & LISGARTEN, N. D. (1957). *Proc. R. Soc. A*, **239**, 93–107.
BRILL, R. & TIPPE, A. (1967). *Acta Cryst.* **23**, 343–345.
COLLINS, J. G. & WHITE, G. K. (1964). *Prog. Low Temp. Phys.* **4**, 450–479.
DANTL, G. (1962). *Z. Phys.* **166**, 115–118.
DANTL, G. (1968). *Phys. Kondens. Mater.* **7**, 390–397.
GIAUQUE, W. F. & STOUT, J. W. (1936). *J. Am. Chem. Soc.* **58**, 1144–1150.
GIBBONS, D. F. (1958). *Phys. Rev.* **112**, 136–143.
GINNINGS, D. C. & CORRUCCINI, R. J. (1947). *J. Res. Nat. Bur. Stand.* **38**, 583–591.
HALTENORTH, H. (1973). Thesis, Technische Universität München.
HARUNA, K., MAETA, H., OHASHI, K. & KOIKE, T. (1986). *J. Phys. C*, **19**, 5149–5154.
IHRINGER, J. & KUESTER, A. (1993). *J. Appl. Cryst.* **26**, 135–147.
JAKOB, M. & ERK, S. (1929). *Wiss. Abh. Phys. Techn. Reichsanst.* **12**, 302–316.
KAHANE, A., KLINGER, J. & PHILIPPE, M. (1969). *Solid State Commun.* **7**, 1055–1056.
KUHARSKY, R. A. & ROSSKY, P. J. (1985). *J. Chem. Phys.* **82**, 5164–5173.
KUHS, W. F. & LEHMANN, M. S. (1986). *Water Sci. Rev.* **2**, 1–65.
KUHS, W. F. & LEHMANN, M. S. (1987). *J. Phys. C*, **48**, 3–8.
LAPLACA, S. & POST, B. (1960). *Acta Cryst.* **13**, 503–505.
LEADBETTER, A. J. (1965). *Proc. R. Soc. A*, **287**, 403–425.
LONG, E. A. & KEMP, J. D. (1936). *J. Am. Chem. Soc.* **58**, 1829–1834.
LONSDALE, K. (1958). *Proc. R. Soc. A*, **247**, 424–434.
LYON, K. G., SALINGER, G. L. & SWENSON, C. A. (1977). *J. Appl. Phys.* **48**, 865–868.
MEGAW, H. D. (1934). *Nature*, **134**, 900–901.
MITZDORF, U. & HELMREICH, D. (1971). *J. Acoust. Soc. Am.* **49**, 723–728.
NOVIKOVA, S. I. (1961). *Sov. Phys. Solid State*, **3**, 129–130.
OKADA, Y. & TOKUMARU, Y. (1984). *J. Appl. Phys.* **56**, 314–320.
ROOT, J. H., EGELSTAFF, P. A. & HIME, A. (1986). *Chem. Phys.* **109**, 437–453.
STRUVE, W. (1845). *Pogg. Ann.* **66**, 298–300.
TIMMERMANS, J., HENNAUT-ROLAND, M. & ROZENTAL, D. (1936). *C. R. Acad. Sci. Paris*, **202**, 1061–1063.
TRUBY, F. K. (1955). *Science*, **121**, 404.
VEGARD, L. & HILLESUND, S. (1942). *Avh. Nor. Vidensk. Akad. Osl. Mat. Nautvidensk. Kl.* **8**, 1–24.
XU, C. H., WANG, C. Z., CHAN, C. T. & HO, K. M. (1991). *Phys. Rev. B*, **43**, 5024–5027.